WHEEL PROFILE DESIGN FOR TARGET CONICITY AND WIDE TREAD WEAR SPREADING

Oldrich POLACH*

*Bombardier Transportation, Winterthur

ABSTRACT

This article deals with design of new wheel tread profile. An interrelationship between the equivalent conicity, contact angle and location of contact area in nominal position, the contact stress and lateral contact spreading is explained and illustrated on examples of measured worn wheel profiles. This relationship has been considered in the proposed method for profile design applied to create new profiles with target conicity and at the same time wide contact spreading. The proposed profiles are suited for vehicles running on straight tracks and/or high power traction vehicles.

Key words: Wheel profile, profile development, wheel wear, tread wear, wear spreading, equivalent conicity.

Nomenclature:

k_y dimensionless proportionality coefficient in the transformation equation of the lateral contact point coordinate from the wheel to the rail profile

R_W radius of wheel cross profile

R_R radius of rail cross profile

y_{WS} lateral wheelset displacement

Y_R lateral coordinate of rail cross profile

Y_W lateral coordinate of wheel cross profile

Y_{W0} lateral coordinate of the contact point on the wheel cross profile in the nominal position

Y_0 lateral offset of the origins of wheel and rail profile coordinate systems

Z_R vertical coordinate of rail cross profile

Z_W vertical coordinate of wheel cross profile

Z_{W0} vertical coordinate of the contact point on the wheel cross profile in the nominal position

Z_0 vertical offset of the origins of wheel and rail profile coordinate systems

γ_0 contact angle between wheel and rail profiles in the nominal position

Δr difference of rolling radii between left and right wheel

λ equivalent conicity

Indices:

i	step of lateral wheelset displacement
l	left
r	right
R	rail
W	wheel
$'$	derivative

1 INTRODUCTION

Contact geometry between wheel and rail or between wheelset and track, respectively, affects the safety against derailment, running stability, forces between wheel and rail in curves, ride comfort, wear of wheels and rails and risk of rolling contact fatigue (RCF). All these aspects should be considered during the assessment of wheel and rail profiles.

A design of new wheel profile well suited for a specific vehicle, track and service conditions can improve running performance, reduce wear and/or avoid wheel or rail damage. The design of wheel or rail profile, respectively, is an important task of wheel/rail contact mechanics. In spite of a large number of publications from this field, this task is still topical. Various methods with different targets and strategies for the development of a new, theoretical wheel profile can be found in publications. There are examples of profile design based on:

- target roll radius difference function [1], [2], [3]
- target contact angle [4]
- wheel profile designed by a lateral stretching of a rail profile [5]
- profile design applying genetic algorithm [6], [7].

The relevance of wheel profile sections can be seen in Fig. 1. The central part around the taping line (tread datum) is relevant to running stability and ride, the part close to the flange root affects the curving performance. Both sides of flange are important from the point of view of safety against derailment.

The development of a new wheel profile design can be a very tedious long term process as shown in the paper by Fröhling [8] describing 7 steps of the wheel profile optimization for freight wagons with self steering bogies within Spoornet (South Africa). The target of the profile optimization differs and is dependent on the; vehicle type, track layout and service conditions, whereas the main target is not always known before the service experience. In the 1980's and 90's, minimized flange wear ("perfect steering") has been supposed to be the optimum allowing significant increase of running distance between the wheel turning or wheelset replacements. To improve the self steering of wheelsets, conformal wheel profiles with sufficiently high rolling radius difference are developed and reported to improve curving performance and to reduce flange wear, see e.g. [9]. In the last decade, RCF comes out as the most important topic and profile optimizations with the aim to reduce the RCF are carried out. Whereas some publications report reduced risk of RCF when using more conformal contact with reduced wheel/rail forces in curves [10], other papers report the optimum between the wheel wear and RCF being achieved by application of less conformal wheel/rail contact geometry with slightly worse curving performance, in combination with flange lubrication [11], [12].

Besides the curving performance, wear and RCF, running stability is another important criterion to be considered during the profile design, because the stability assessment is one of the most important tasks of running dynamics [13], [14]. The stability requirements are usually contradictory to the curving requirements. Whereas a more conformal contact and higher difference of rolling radii improves the self steering ability of wheelsets, the same considers a higher risk of the safety relevant self excited bogie oscillations called instability in railway applications.

Even if the required targets for stability and curving are reached for the theoretical profile, the shape of the wheel profile and consequently the running performance can change due to wear. A common approach is to use a typical worn wheel profile as a basis for the development of a new wheel profile under the assumption that the "worn type" profile will keep its form in service. The lateral shape of wheel profile, however, rather seldom keeps its form with wear. Even a "worn type" design wheel profile based on a large number of measured worn wheel profiles often changes its tread shape due to tread wear, mainly at vehicles running on prevailing straight track and/or at high power traction vehicles. The tread wear due to traction creep increases mainly under low adhesion conditions. To transfer large traction forces under insufficient adhesion conditions, modern vehicles maintain large creep values by advanced traction control, leading to wheel tread conditioning and an increase of traction force. However, a large creep between wheel and rail changes the wear from mild or severe to a catastrophic wear [15], and wheel conditioning by sanding in wet conditions increases the wheel wear by a factor of up to 10 compared to dry conditions without sanding [16]. An increasing conformity of a wheel profile together with increasing conicity due to prevailing tread wear can hardly be avoided at these vehicles.

Local tread wear can be reduced by applying a new design wheel profile with a wider wear spreading across the profile shape. This article deals with the development of such new, design tread profile with regard to stability requirements, i.e. to target conicity. The paper is structured as follows: In Chapter 2, the relationship between the contact angle, conformity, equivalent conicity and the contact spreading during lateral wheelset displacement is explained. Chapter 3 presents a case study which illustrates the effect of contact geometry on the contact spreading comparing measured profile development of different theoretical wheel profiles applied on a vehicle running with large traction creep on prevailing straight tracks. A new wheel profile design with a wide contact spreading and target conicity together with profiles examples related to the investigated case study are presented in Chapter 4. Chapter 5 contains conclusions and outlook.

2 INTERRELATIONSHIP BETWEEN THE NOMINAL CONTACT ANGLE, CONFORMITY AND EQUIVALENT CONICITY

A well known parameter largely used to describe the wheel/rail contact geometry in railway applications is the equivalent conicity. There are different methods for calculation of equivalent conicity, see [17], [18]. We will use equivalent linearisation [17] and harmonic linearisation [19], which both assume periodic wheelset movement with a specified amplitude.

The equivalent conicity is an important parameter related to a vehicle's running dynamics performance and mainly to running stability. A high equivalent conicity can lead to a risk of unstable running of bogies, whereas a very low conicity can lead to a combined oscillation of vehicle body and bogies due to a resonance between the bogies' waving movement and an eigenmode of the vehicle's body. The equivalent conicity can

vary in dependency of wheelset amplitude whereby the vehicle's running behaviour can differ dependent of the shape of the equivalent conicity function [20]. The equivalent conicity for wheelset lateral displacement amplitude of 3 mm is usually used for the wheel/rail contact geometry assessment in railway application [21]. Typical equivalent conicities for a wheelset amplitude of 3 mm accompanied with a smooth running behaviour lie in range of 0.10 - 0.25.

The equivalent conicity is determined by the rolling radius difference due to lateral wheelset displacement. The rolling radius difference is dependent on the contact angle between wheel and rail and on the local curvatures of wheel and rail profiles. The linearisation of wheel/rail contact geometry described by Mauer [19] can be simplified for small contact angles (see Fig. 2) as follows:

$$\lambda \approx \gamma_0 \frac{R_W}{R_W - R_R} \qquad (1)$$

Consequently, the same difference of rolling radii and hence a similar level of equivalent conicity can be achieved:

- either by variation of the wheel tread contact angle; the consequence is a lateral shift of the nominal wheel/rail contact point,
- or by variation of the wheel profile arc radius; whereby a decrease of profile radius leads to a more conformal contact with larger lateral movement of the contact point and wider contact spreading.

The conicity level of a newly designed wheel profile can therefore be influenced by both: the nominal contact angle and the conformity of the tread profile section, see Fig. 3. Other parameters as lateral location of the contact area on the wheel profile, contact size, normal stress and contact spreading during the lateral wheelset displacement are related to the nominal contact angle and conformity.

A reduction of the wheel profile radius R_W closer to rail profile radius R_R increases the lateral movement of contact point and thus enlarges the contact spreading and vice versa. Increased conformity is accompanied with lateral enlargement of the contact size and hence lower normal stress and at the same time increasing rolling radius difference and equivalent conicity. A shifting of the nominal contact to the field side leads to a reduction of the contact angle and consequently lowering of equivalent conicity, a shifting of the contact to the flange side goes ahead with an increase of the contact angle and raising equivalent conicity.

This interrelationship between the position of the wheel/rail contact point for the nominal parameters, contact angle, conformity, equivalent conicity and contact spreading should be considered during a design of new wheel profile because it affects the wear distribution and consequently the stability of profile shape due to wear and also the smoothness of running performance with mileage and wheel wear.

3 A CASE STUDY: CONTACT SPREADING AND WHEEL WEAR

The relationship described in the previous chapter is illustrated by examples of newly developed wheel profiles tested in service on a tractive vehicle running predominantly on straight lines.

The originally applied wheel profile S1002 combined with rail inclination 1:40 resulted in a very low conicity below 0.1 due to a wider flange clearance of the investigated broad gauge wheelset/track system compared to nominal parameters of normal gauge, see Fig. 4. A degraded running performance was observed

infrequently, and was identified as low frequency oscillations related to very low conicity. Because of conicity increasing due to traction creep, this phenomenon was observed at vehicles with new or slightly worn wheels.

To avoid vehicle service work at very low conicity, a new design wheel profile PF000 was developed and tested. This profile was derived from a few measured worn wheel profiles and adapted to achieve the target equivalent conicity higher than 0.15 for an amplitude of 3 mm for the nominal as well as slightly increased track gauge values. The tread of this profile consists of radii 400 and 120 mm. After some time in service, a tread wear concentrated on rather small area was observed. The analysis of wheel/rail contact geometry for lateral wheelset displacement (Fig. 5) showed for nominal parameters the contact in the wheel profile coordinate system at approximately -9 mm (i.e. 9 mm from the taping line in direction to the flange), a small contact spreading and rather small contact area. An alternative wheel profile PF602 has been developed by modification of the profile's arc radii to 380 and 90 mm and reducing the nominal contact angle. This resulted in a contact at -2 mm and a wider contact spreading at similar equivalent conicity level, see Fig. 6.

A development of the wheel profiles PF000 and PF602 due to wear at large traction creep during the winter period can be seen in the bottom diagrams in Fig. 5 and 6. The wheel profile measurements demonstrate the influence of wheel profile on the wear spreading and confirm wider wear spreading at the profile PF602 compared with the profile PF000.

The wear spreading across the wheel profile when running on straight lines is determined by the lateral movement of the wheel/rail contact patch. Estimating a stochastic lateral wheelset displacement with normal Gaussian distribution, the wear distribution across the wheel tread profile can be represented by a probability of the normal distribution with a suited standard deviation of wheelset displacement y_w displayed as a function of the position of contact point (centre of the contact patch) on the wheel profile for the relevant wheelset displacement, see Fig. 7. Fig. 8 represents this estimated wear distribution for the profiles S1002, PF000 and PF602 and for a standard deviation of wheelset amplitude 4.6 mm. Compared with measured wheel wear due to traction creep, the wear estimation shows a good qualitative agreement regarding the location of maximum wear and the asymmetry of the wear distribution. The qualitative difference on the field side is related to the wear due to tread brake not considered in this assessment. This wear estimation, however, is only a rough prediction, suited for a service on lines with small percentage of curves.. It can be used in conditions, in which the rails maintain certain shapes with very small variation, e.g. using one nominal rail profile maintained regularly by grinding.

The presented case study using wheel profiles consisting of few arc sections demonstrated that an improved wheel profile can shift and enlarge the wear spreading laterally over the wheel profile and thus reduce the local tread wear. A comparison of measured wheel profiles during the winter and summer period, however, showed that in the presented case a severe wheel wear at low adhesion conditions, with large traction creep and intensive wheel conditioning, can not be fully compensated optimizing the wheel profile.

Because of limitations of the wheel profile design consisting of few arc sections, a possible further increase of contact spreading using a wheel profile with continuously changing curvature has been investigated. Chapter 4 shows suitable methods for a design of such new wheel tread profiles and compares the resulted wheel profiles with the profiles presented above.

4 WHEEL PROFILE DESIGN FOR A WIDE CONTACT SPREADING

4.1 Wheel profile design by stretching of proven wheel profile

In the presented case study, a proven system (wheel profile S1002, rail profile UIC 60, rail inclination 1:40) changed its properties due to increased nominal clearance of the investigated broad track gauge compared to the normal gauge system. As a consequence, equivalent conicity changed to very low value. Because the profiles consisting of few arc sections showed rather small spreading compared to the properties known from the normal gauge, a new tread profile was created by stretching the tread section of the profile S1002 according to the gauge clearance increase. The resultant wheel profile PF603 has a continuously increasing wheel profile radius in the wheel/rail contact point. For nominal wheelset/track parameters, the location of the contact area on the wheel profile is at 2.5 mm to the field side from the taping line.
The profile PF603 shows similar contact geometry as known from the contact of wheel profile S1002 with rail UIC 60 1:40, normal track gauge and nominal parameters, see Fig. 9. Whereas the equivalent conicity as function of wheelset amplitude increases for PF000 and PF602, the profile PF603 shows a decreasing equivalent conicity function for small wheelset amplitudes considering the rigid contact and constant equivalent conicity applying elastic contact. A wide contact spreading and large contact patches are illustrated in Fig. 9.

4.2 Wheel profile design based on specified contact distribution

To achieve a wide contact spreading and target conicity level without a possibility to use experience with other proven wheel profile, a method for wheel profile design based on a specified distribution of contact points over the wheel profile has been developed. This method is suited for vehicles running prevailing on straight lines and/or with heavy traction forces, leading to a rapid change of wheel tread shape after the turning. The method may be applied to conditions, in which the population of rails maintain certain shapes with very small variations, e.g. if the network contains one type of rail which is maintained regularly by grinding.
The proposed design of wheel profile tread is based on the specified rail profile. This rail profile in the inclination as built in on track is described by a discrete function in the coordinate system with the origin in the centre of the top of rail head

$$Z_R = f(Y_R) \tag{2}$$

We search for a wheel profile described by a function

$$Z_W = f(Y_W) \tag{3}$$

in the wheel coordinate system with the origin in the taping line (tread datum) of this profile functions.
The track gauge and the lateral wheel distance in the nominal position determine the offset of the origins of the rail coordinate systems and wheel coordinate system in lateral Y_0 or vertical Z_0 direction, respectively.
The following assumptions are made:

1. The wheel and rail are both rigid bodies.

2. The rail profile is continuous and convex.
3. The left and right wheel and rail profiles are symmetric.
4. The contact between wheel and rail is represented by a contact point.
5. The wheelset roll angle around the longitudinal axis due to lateral wheelset displacement is small and can be neglected.

The contact spreading can be described by the contact point movement ΔY_W due to change of wheelset displacement Δy_{WS}

$$\frac{\Delta Y_W}{\Delta y_{WS}} = Y'_W\left(y_{WS}\right) \tag{4}$$

For the proposed contact spreading Y'_W on the wheel profile, the distribution of Y_W-coordinate of the wheel contact points can be calculated as

$$Y_W\left(y_{WS}\right) = \int Y'_W\left(y_{WS}\right)\, d\, y_{WS} \tag{5}$$

Let's consider the selected distribution of contact points Y_W on the wheel profile and a specified wheel rolling radius difference function as input parameters, whereas the distribution of the contact points on the rail profile is not prescribed. To achieve continuous spreading, lateral distribution of the contact points on the rail profile can be assumed proportional to the contact point distribution on the wheel profile. The wheel contact points can be transformed to the contact points on the rail by the equation

$$Y_R\left(y_{WS}\right) = Y_W\left(y_{WS}\right) + k_y y_{WS} + Y_0 \tag{6}$$

In the contact point between wheel and rail, the tangents of wheel and rail profiles are identical. Thus, from the derivative of the rail contact point coordinate $Z'_R(Y_R)$ we can get the derivative of the wheel contact point coordinate $Z'_W(Y_W)$ for each step i of the wheelset lateral displacement y_{WS}

$$Z'_W\left(Y_W\right)\Big|_{y_{WS_i}} = Z'_R\left(Y_R\right)\Big|_{y_{WS_i}} \tag{7}$$

The wheel profile coordinate Z_W can then be obtained as

$$Z_W = \int Z'_W\, dY_W \tag{8}$$

The equivalent conicity is proportional to rolling radius difference, which can be calculated subtracting the vertical coordinates of contact points on the left and right wheel

$$\Delta r\left(y_{WS}\right) = \left(Z_{Rl} - Z_{Wl}\right) - \left(Z_{Rr} - Z_{Wr}\right) \tag{9}$$

Let's consider the equations (4) to (8) for the right rail and wheel. Because of mirroring of symmetrical rail and wheel profiles on left and right side, the coordinate of the left wheel profile can then be calculated by the same equations setting Y_0 and y_{WS} with the opposite sign

$$Y_{0l} = -Y_{0r} \tag{10}$$

$$y_{WS\,l} = -y_{WS\,r} \tag{11}$$

The equations (6) and (8) for left and right wheel and equation (9) can hence be used to calculate unknown quantities Y_{Rr}, Y_{Rl}, Z_{Wr}, Z_{Wl}, k_y.

The coefficient k_y is related to rolling radius difference and can be used to adjust the target equivalent conicity level. Thus, a more simple process of the profile design generation can be applied as follows.

The profile coordinates are calculated for one profile only using estimated coefficient k_y, e.g. $k_y = 1$. To create a new wheel profile, as first, the contact point for the nominal wheelset position $y_{WS} = 0$ is selected. The choice of the nominal contact point affects the value of nominal contact angle and the lateral position of the nominal contact on the wheel and rail profiles.

The wheel profile is then calculated by the integration of (8). The first integration starts from the nominal contact point Y_{W0} to the left, the second from the point Y_{W0} to the right. If the resultant equivalent conicity differs from the specified value, the conicity can then be adjusted by a reduction of the coefficient k_y if the conicity of the first profile is too low or by an increase of this coefficient if the conicity is too high, respectively. The choice of the contact point distribution and of the proportionality coefficient k_y is certainly limited by the length of the wheel tread section and the rail width before the flange root contacts the rail gauge corner. These constraints limit the possible profile shape and properties. The resultant tread profile is then extended with a flange and field side sections identical or similar to the original profile.

The proposed method has been applied for the wheelset/track system described in Chapter 3 to calculate a new profile with a large spreading of the contact points on the wheel profile and at the same time equivalent conicity > 0.1. The resultant wheel profile PF810 has in the nominal position the location of the contact area on the wheel profile at 5.6 mm to the field side from the taping line. The wheel/rail contact is characterized by a wide contact spreading and an equivalent conicity slightly growing with increasing wheelset displacement amplitude, see Fig. 10.

4.3 Comparison of proposed profiles

Fig. 11 shows the contact patch area and the maximum normal contact stress between wheel and rail in function of wheelset displacement of the proposed profiles PF603 and PF810 and a comparison with the profiles PF000 and PF602 investigated in Chapter 3. The results were calculated using the tool RSGEO [22] which considers elastic contact and non-elliptical contact patches, however considering linear contact elasticity. The maximum normal stress is represented by the maximum stress of an equivalent contact ellipse with the area of the non-elliptical contact patch.

The profiles PF603 and PF810 demonstrate an increased contact area and significantly reduced maximum stresses compared with the profile PF000 and partly also in comparison with the profile PF602. The estimated wear distribution of the proposed profiles presented in Fig. 11 shows wider spreading across the profile against the profile PF000 used in the first trial. The profile PF810 exhibits the largest distribution while fulfilling the requirement for equivalent conicity > 0.1.

Both profiles PF603 and PF810 possess similar shape and properties, in spite that they have been developed using different methods. This demonstrates that a further optimization of wear spreading together with fulfilment of the equivalent conicity requirement is hardly possible.

5 CONCLUSIONS AND OUTLOOK

When designing a new wheel profile, the interrelationship between the equivalent conicity, contact angle and location of contact area in nominal position, contact stress and lateral contact spreading should be considered. This interrelationship is explained and illustrated on examples of measured worn wheel profiles.

The paper presents possible methods for a design of wheel profile with continuously changing curvature. The presented examples confirm an improvement using proposed profile design methodologies in comparison to an arc profile design created by trial and error.

For vehicles characterized by dominating tread wear, the wear distribution can be estimated based on the lateral position of the contact points on the profile shape. This simplified wear estimation can be used to select the optimum wear distribution of the contact points on the wheel profile which can then be applied to create the new wheel profile.

The proposed methodology of the wheel profile design based on simplified wear estimation can be combined with simulations of wear development under realistic conditions presented e.g. by Enblom [23]. To carry out these simulations for vehicles with severe traction wear, the simulation model necessitates an extension with a traction control model and an extended creep force model as described by the author in [24]. Further research studies would also be required for the identification of wear coefficients (wear map) and verification of simulations of profile development due to traction wear by comparison of simulations and measurements.

REFERENCES

[1] R.E. Smith and J. Kalousek: A design methodology for wheel and rail profiles for use on steered railway vehicles. *Wear*, 1991, vol. 144, pp. 329-342

[2] D. Nicklisch: *Contact surface between a rail and the wheel of a railway vehicle*. European Patent Office, EP 1091044, 2000

[3] T. Lack and J. Gerlici: Iterational method for railway wheel tread profile design. *XVIII Konferencja naukowa - Pojazdy Szynowe, Politechnika Slaska – Komitet transportu PAN. Materialy konferencyjne, Tom I*, pp. 137-149. Katowice – Ustroń, 2008

[4] G. Shen, J.B. Ayasse, H. Chollet and I. Pratt: A unique design method for wheel profiles by considering the contact angle function. *Proc. Instn. Mech. Engrs., Part F.: J. Rail and Rapid Transit*, 2003, vol. 217, pp. 25-30

[5] J.F. Leary, S.N. Handal and B. Rajkumar: Development of freight car wheel profiles — a case study. *Wear*, 1991, vol. 144, pp. 353-362

[6] I. Persson and S.D. Iwnicki: Optimisation of railway wheel profiles using a genetic algorithm. *Vehicle System Dynamics, Supplement*, 2004, vol. 41, pp. 517-526

[7] M. Novales, A. Orro, and M.R. Bugarín: Use of a genetic algorithm to optimize wheel profile geometry. *Proc. Instn. Mech. Engrs., Part F.: J. Rail and Rapid Transit*, 2007, vol. 221, pp. 467-476

[8] R. Fröhling: Vehicle/track interaction optimisation within Spoornet. In: K. Popp and W. Schiehlen, (Eds.), *System dynamics and long-term behaviour of railway vehicles, track and subgrade*, pp. 17-34. Springer-Verlag, Berlin Heidelberg New York, 2003

[9] W. You, H. Hur and H. Kim: A design of new shape arc-type wheel profile to reduce flange wear. *Proceedings of the 7th International Conference on Contact Mechanics and Wear of Rail/Wheel Systems (CM 2006)*, Brisbane, Australia, September 24-26, 2006, pp. 681-687

[10] H. Wu: Control of wheel/rail wear and RCF. *Proceeding of the International Heavy Haul Conference*, Kiruna, Sweden, June 11-13, 2007, pp. 607-616

[11] J.R. Evans, T.K.Y. Lee and C.C. Hon: Optimising the wheel/rail interface on a modern urban rail system. *Vehicle System Dynamics, Supplement*, 2008, vol. 46, pp. 119-127

[12] I.Y. Shevtsov, V.L. Markine and C. Esveld: Design of railway wheel profile taking into account rolling contact fatigue and wear. *Wear*, 2008, vol. 265, pp. 1273-1282

[13] O. Polach: On non-linear methods of bogie stability assessment using computer simulations. *Proc. Instn. Mech. Engrs., Part F.: J. Rail and Rapid Transit*, 2006, vol. 220, pp. 13-27

[14] O. Polach: Influence of wheel/rail contact geometry on the behaviour of a railway vehicle at stability limit. *Proceedings ENOC-2005*, Eindhoven University of Technology, The Netherlands, 7-12 August 2005, pp. 2203-2210
[15] R. Lewis and U. Olofsson: Mapping rail wear regimes and transitions. *Wear*, 2004, vol. 257, pp. 721-729
[16] R. Lewis and R.S. Dwyer-Joyce: Wear at the wheel/rail interface when sanding is used to increase adhesion. *Proc. Instn. Mech. Engrs., Part F.: J. Rail and Rapid Transit*, 2006, vol. 220, pp. 29-41
[17] EN 15302: *Railway application — Method for determining the equivalent conicity*. CEN, Brussels, March 2008
[18] F. Braghin, S. Bruni and S. Alfi: Critical velocity of railway vehicles. *Proceedings of the 10th Mini Conference on Vehicle System Dynamics, Identification and Anomalies (VSDIA 2006)*, 6-8 November 2006, Budapest, Hungary
[19] L. Mauer: The modular description of the wheel to rail contact within the linear multibody formalism. In: J. Kisilowski and K. Knothe (Eds.): *Advanced Railway Vehicle System Dynamics*, Wydawnictwa Naukowo-Techniczne, Warsaw, 1991, pp. 205-244
[20] O. Polach: Characteristic parameters of nonlinear wheel/rail contact geometry. Paper No. 95, *Proceedings of the 21st IAVSD Symposium*, Stockholm, 17-21 August 2009
[21] EN 14363: *Railway applications—Testing for the acceptance of running characteristics of railway vehicles—Testing of running behaviour and stationary tests.* CEN, Brussels, 2005
[22] *Program RSGEO*. Description available at http://www.argecare.com/products.htm (assessed 1.7.2009 at 11:25)
[23] R. Enblom: *On simulation of uniform wear and profile evolution in the wheel – rail contact*. Doctoral thesis, Royal Institute of Technology (KTH), Stockholm, 2006
[24] O. Polach: Creep forces in simulations of traction vehicles running on adhesion limit. *Wear*, 2005, vol. 258, pp. 992-1000

Figures

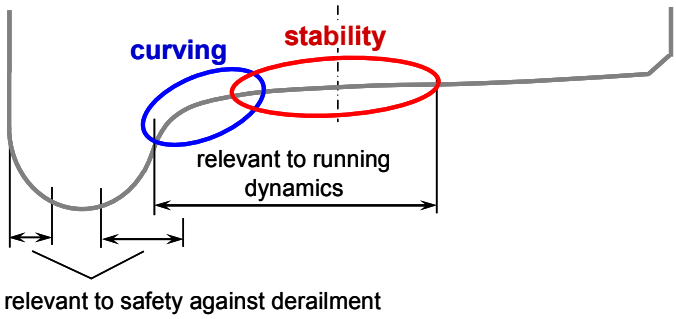

Figure 1. Relevance of wheel profile sections regarding running dynamics.

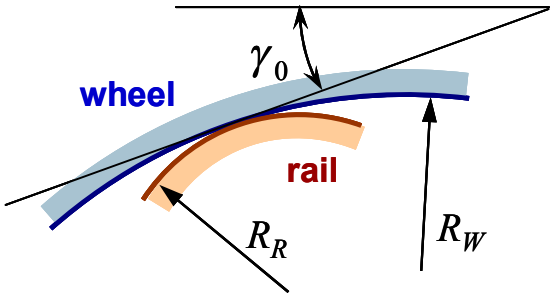

Figure 2. Simplified representation of wheel/rail contact.

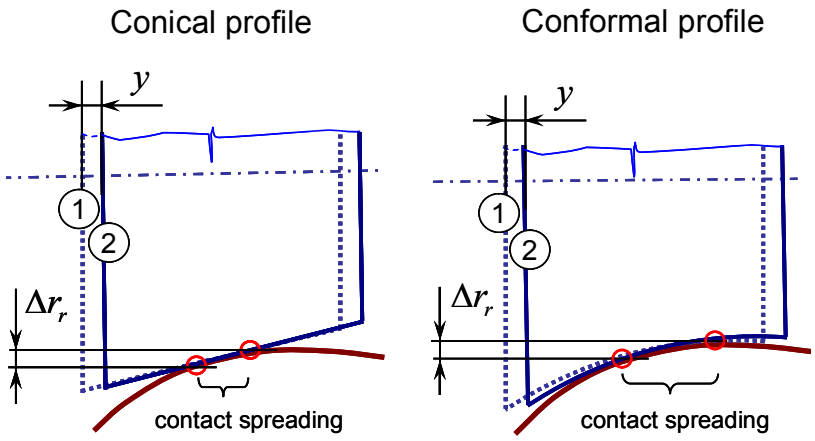

Figure 3. Relationship between conformity and contact spreading for a wheelset movement from position 1 to position 2.

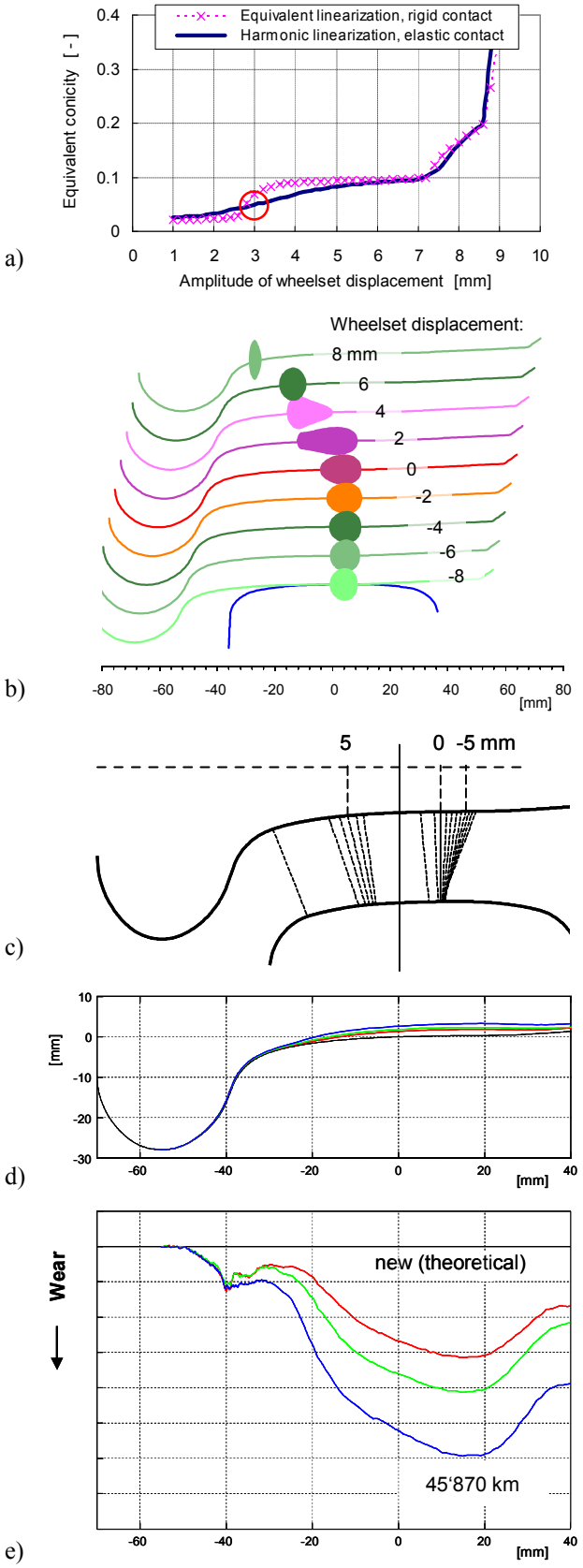

Figure 4. Wheel profile S1002 (from top down):
a) Equivalent conicity
b) Shapes and positions of wheel/rail contact patch (elastic contact)
c) Positions of wheel/rail contact points (rigid contact)
d) Measured wheel profiles
e) Vertical difference compared to the theoretical profile

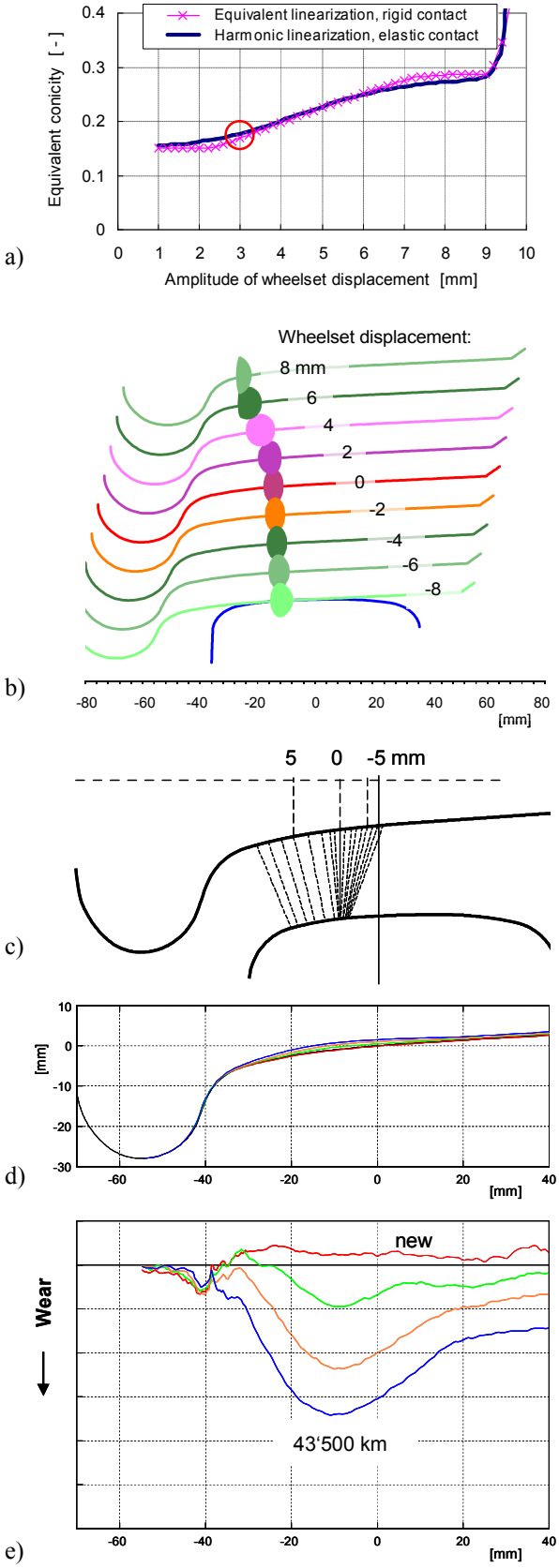

Figure 5. Wheel profile PF000 (from top down):
a) Equivalent conicity
b) Shapes and positions of wheel/rail contact patch (elastic contact)
c) Positions of wheel/rail contact points (rigid contact)
d) Measured wheel profiles
e) Vertical difference compared to the theoretical profile

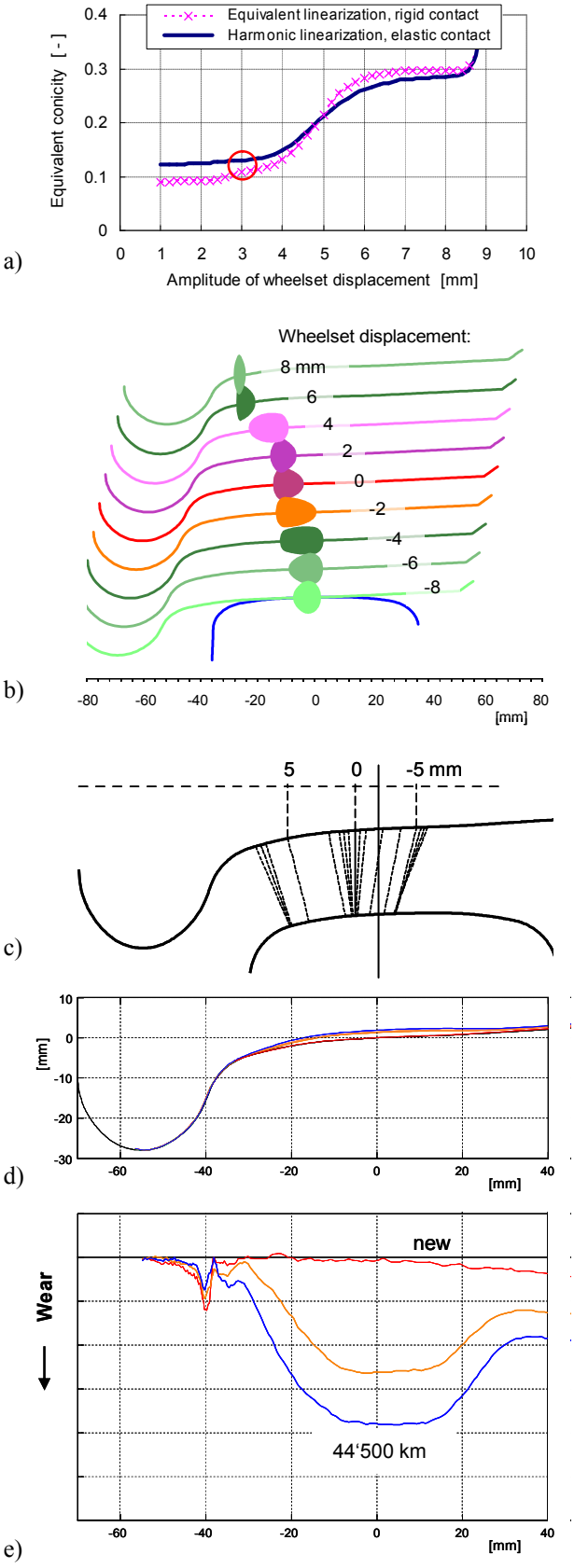

Figure 6. Wheel profile PF602 (from top down):
a) Equivalent conicity
b) Shapes and positions of wheel/rail contact patch (elastic contact)
c) Positions of wheel/rail contact points (rigid contact)
d) Measured wheel profiles
e) Vertical difference compared to the theoretical profile

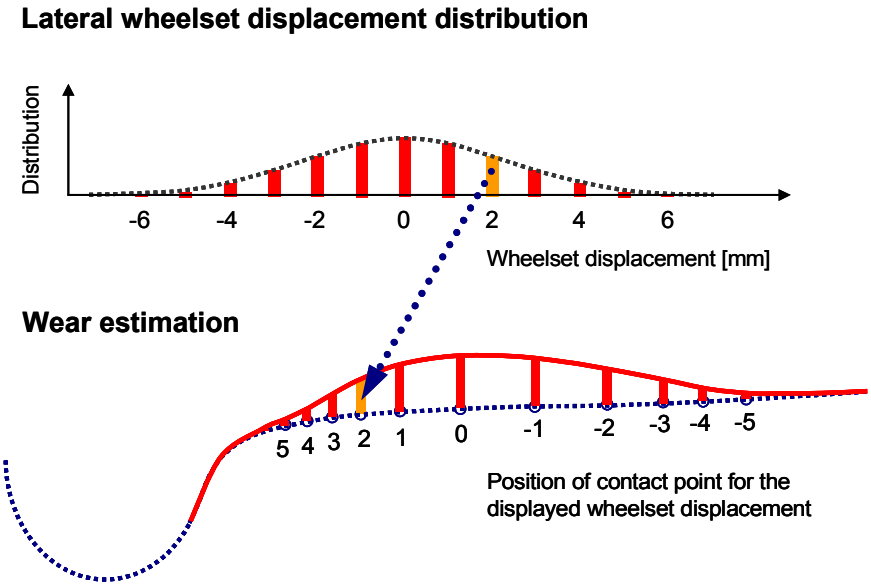

Figure 7. Principle of wheel wear estimation on straight tracks.

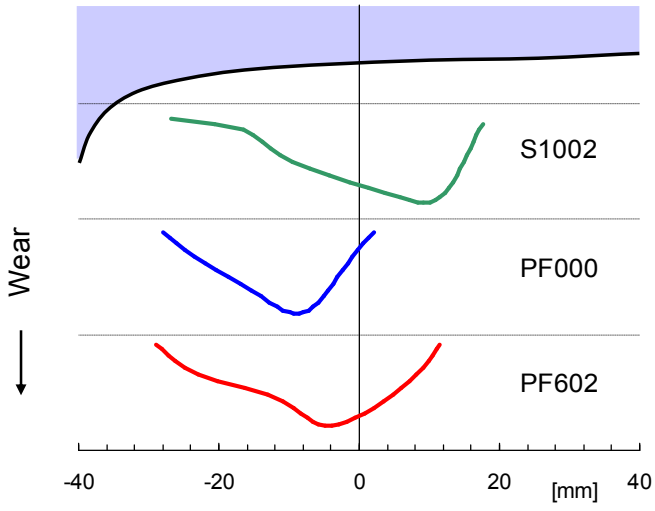

Figure 8. Estimated wear distribution across the investigated profiles.

a)

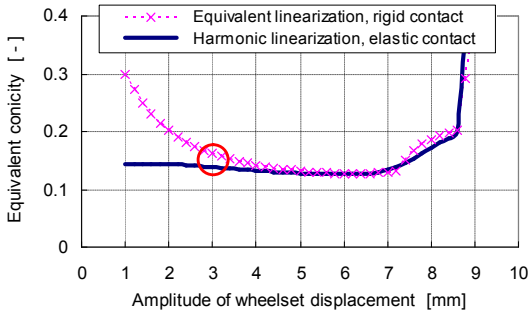

b)

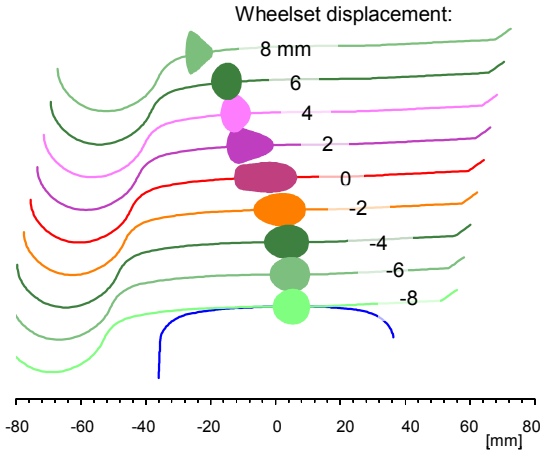

c)

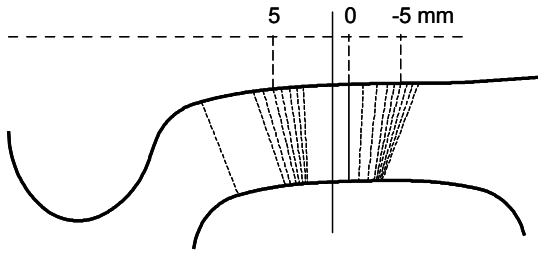

Figure 9. Wheel profile PF603:
a) Equivalent conicity
b) Shapes and positions of wheel/rail contact patch (elastic contact)
c) Positions of wheel/rail contact points (rigid contact)

a)

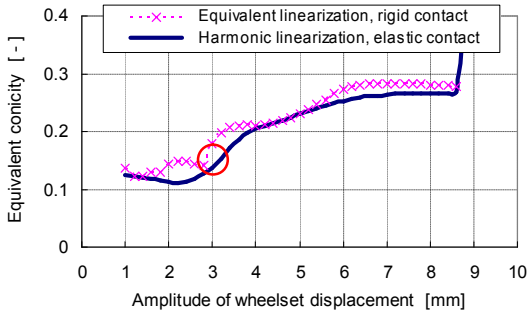

b)

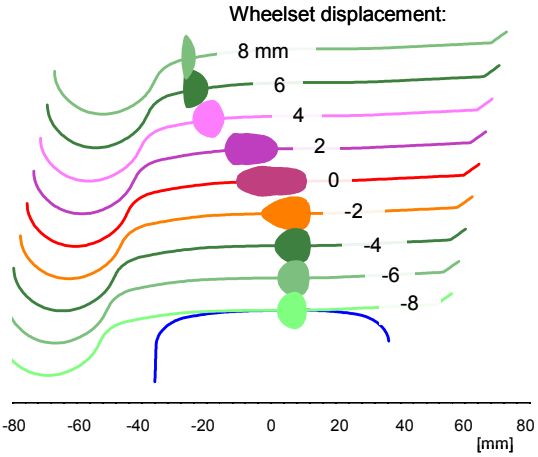

c)

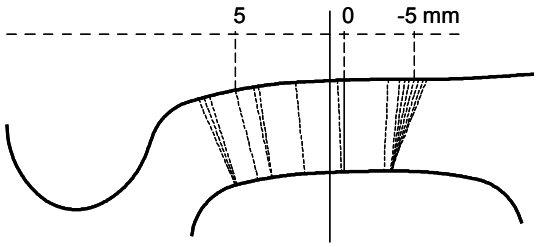

Figure 10. Wheel profile PF810:
a) Equivalent conicity
b) Shapes and positions of wheel/rail contact patch (elastic contact)
c) Positions of wheel/rail contact points (rigid contact)

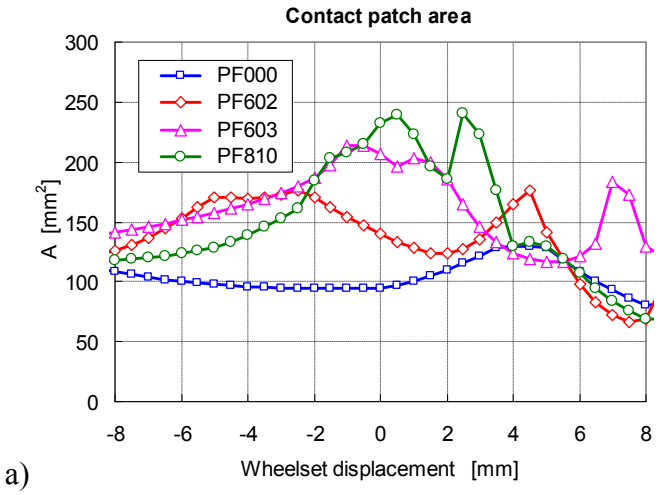

a)

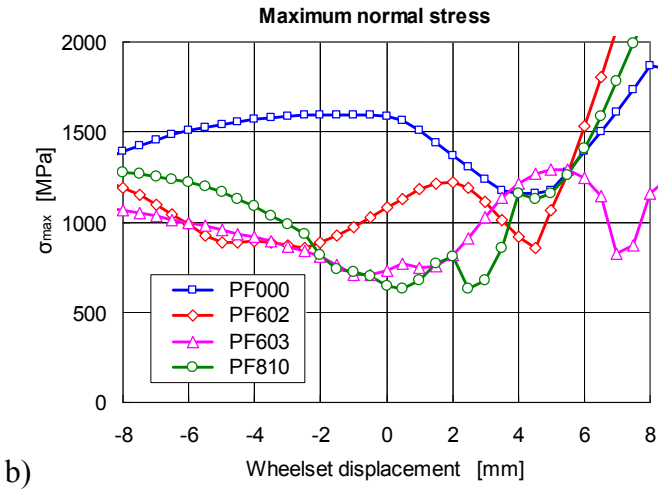

b)

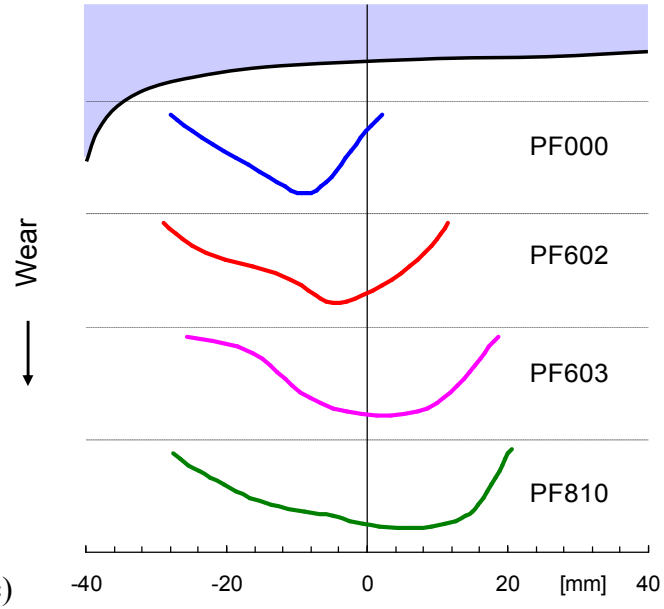

c)

Figure 11. Comparison of profiles PF000, PF602, PF603 and PF810:
a) Contact patch area
b) Maximum normal stress
c) Estimated wear distribution across the wheel profile